Anomalous C-V response correlated to relaxation processes in TiO_2 thin film based-metal-insulator-metal capacitor: Effect of titanium and oxygen defects

A. Kahouli' , C. Marichy' , A. Sylvestre, and N. Pinna

Citation: Journal of Applied Physics **117**, 154101 (2015); doi: 10.1063/1.4917531
View online: http://dx.doi.org/10.1063/1.4917531
View Table of Contents: http://aip.scitation.org/toc/jap/117/15
Published by the American Institute of Physics

JOURNAL OF APPLIED PHYSICS **117**, 154101 (2015)

Anomalous C-V response correlated to relaxation processes in TiO_2 thin film based-metal-insulator-metal capacitor: Effect of titanium and oxygen defects

A. Kahouli,[1,2,a)] C. Marichy,[3,b)] A. Sylvestre,[2] and N. Pinna[4]
[1]*Laboratory for Materials, Organization and Properties (LabMOP), 2092 Tunis, Tunisia*
[2]*University Grenoble Alpes, G2Elab, F 38000 Grenoble, France*
[3]*Complexo de Laboratórios Tecnológicos, Universidade de Aveiro/CICECO, Campus Universitario de Santiago, 3810 193 Aveiro, Portugal*
[4]*Humboldt Universität zu Berlin Institut für Chemie*

(Received 17 October 2014; accepted 2 April 2015; published online 15 April 2015)

Capacitance-voltage (C V) and capacitance-frequency (C f) measurements are performed on atomic layer deposited TiO_2 thin films with top and bottom Au and Pt electrodes, respectively, over a large temperature and frequency range. A sharp capacitance peak/discontinuity (C V anomalous) is observed in the C V characteristics at various temperatures and voltages. It is demonstrated that this phenomenon is directly associated with oxygen vacancies. The C V peak irreversibility and dissymmetry at the reversal dc voltage are attributed to difference between the Schottky contacts at the metal/TiO_2 interfaces. Dielectric analyses reveal two relaxation processes with degeneration of the activation energy. The low trap level of 0.60 0.65 eV is associated with the first ionized oxygen vacancy at low temperature, while the deep trap level of 1.05 eV is associated to the second ionized oxygen vacancy at high temperature. The DC conductivity of the films exhibits a transition temperature at 200 °C, suggesting a transition from a conduction regime governed by ionized oxygen vacancies to one governed by interstitial Ti^{3+} ions. Both the C V anomalous and relaxation processes in TiO_2 arise from oxygen vacancies, while the conduction mechanism at high temperature is governed by interstitial titanium ions. © *2015 AIP Publishing LLC*.
[http://dx.doi.org/10.1063/1.4917531]

I. INTRODUCTION

Owing to its remarkable optical and electronic properties, titanium dioxide (TiO_2) has extensively studied for numerous applications.[1,2] In particular, TiO_2 thin films are highly attractive for capacitor and microelectronic applications because of their high dielectric constant, with reported values ranging from 18 to 80.[3] Its variability is generally explained by the dependence of the permittivity on the crystalline phase, deposition method and process parameters of the TiO_2. Various techniques such as thermal[4] or anodic oxidation,[5] electron beam evaporation,[6] chemical vapor deposition (CVD),[7] plasma-enhanced chemical vapor deposition,[8] sol-gel methods,[9] reactive sputtering methods,[10,11] and atomic layer deposition (ALD)[12–14] have been reported for TiO_2 thin film fabrication. Among them, ALD seems highly suitable for obtaining conformal films with uniform thickness even at low temperatures,[15,16] allowing the manufacturing of insulator films with desired and reproducible properties. ALD growth proceeds layer by layer without gas phase reaction, permitting control of film thickness at the atomic scale. A crucial issue is the unwanted incorporation of impurities into the film, especially in the case of chemical deposition processes such as ALD and CVD. Indeed, unreacted ligands may remain, causing, for instance, residual carbon and hydrogen impurities when using titanium alkoxide and halides (e.g., Cl) when using titanium halide (e.g., $TiCl_4$) precursors. Such impurities induce additional lattice defects to the common ones, leading to lattice distortion, degradation of crystallinity, and insertion of additional trap states into the dielectric.[12] The reduction or oxidation of Ti ions represents another impurity source. The appearance of different stable oxidation states of Ti such as Ti^{3+} and Ti^{4+} is commonly observed and these act as electron donors and high leakage paths.[17]

In the present work, the defect levels, capacitance voltage (C V) anomalous behaviour, and dielectric properties of ALD TiO_2 thin film used in metal-insulator-metal (MIM) structures are reported. The influence of defects on the relaxation and conductivity mechanisms is discussed and the observed anomalous C V behavior explained.

II. EXPERIMENTAL

After standard cleaning of the Pt/Ti/SiO_2/Si substrates, 46 nm-thick amorphous TiO_2 film was deposited on the Pt electrode by ALD. The deposition was carried out at 200 °C in a home-made reactor working in exposure mode using titanium isopropoxide and acetic acid as the metal and oxygen source, respectively. The full experimental details can be found in Ref. 18. A top gold electrode of 2 mm in diameter was then deposited on the sample by sputtering.

The dielectric properties and capacitance-voltage characteristics of the film were measured using a Novocontrol BDS 20 over a wide temperature and frequency range at

a)Author to whom correspondence should be addressed. Electronic mail: kahouli.kader@yahoo.fr.
b)Present address: LMI, CNRS UMR 5615, Université Lyon 1, 22 av. Gaston Berger Bât. Berthollet, 69622 Cedex Villeurbanne, France.

several applied dc voltages. A low alternating voltage signal of 100 mV was used for the dielectric and electrical measurements.

III. RESULTS AND DISCUSSION

As previously reported for binary oxides, with the exception of SiO_2 which exhibits a negative parabolic form,[19,20] the *C V* characteristics of ALD TiO_2 at low temperature (Fig. 1(a)) displayed a positive parabolic form with a shape independent of the voltage sweep direction. The nonlinearity of the MIM capacitor increased with progressively rising voltage at each measurement temperature. In Fig. 1(b), the *C V* characteristics of the film changed abruptly as the temperature was increased, especially from −25 °C, with appearance of a peak that progressively rose and shifted to higher voltage. Peak saturation was reached between 60 °C and 75 °C and was followed by a drop in intensity and slow shift to lower voltage at higher temperature (Fig. 1(c)). A decrease in the *C V* curves at positive voltage was also observed with increase temperature. Negative capacitance values were obtained above 100 °C and at voltage <−2.5 V, as visible in Fig. 1(c).

The C-V values also increased with temperature up to −50 °C in the whole investigated voltage range, while at higher temperature, starting from −25 °C, only the negative voltage part was impacted by a capacitance increase, the capacitance remaining almost constant in positive voltage region. From 62.5 °C, the capacitance began to decrease in both the negative and positive voltage range, even though the positive curve was less dependent on voltage and temperature than the negative one. This can be attributed to presence of dominating positive charges. Binary oxides are known to be dielectric materials with oxygen defects in their structure, so positive oxygen vacancies may be the origin of the observed capacitance anomaly. Indeed, nonlinearities noted in MIM capacitors have already been attributed to film oxygen content and oxygen vacancies.[21]

The reversibility of the TiO_2-based MIM capacitor was investigated, and the results are illustrated in Fig. 2. At low temperatures up to −50 °C, the clearly parabolic C-V characteristics were reversible, while from −25 °C irreversibility occurred owing to the appearance of a capacitance peak. With increasing temperature, two capacitance peaks appeared during the voltage sweep from positive to negative voltage (Figs. 2(c) 2(e)), whereas only one was observed during the opposite sweep (Figs. 2(c) and 2(d)). This irreversibility

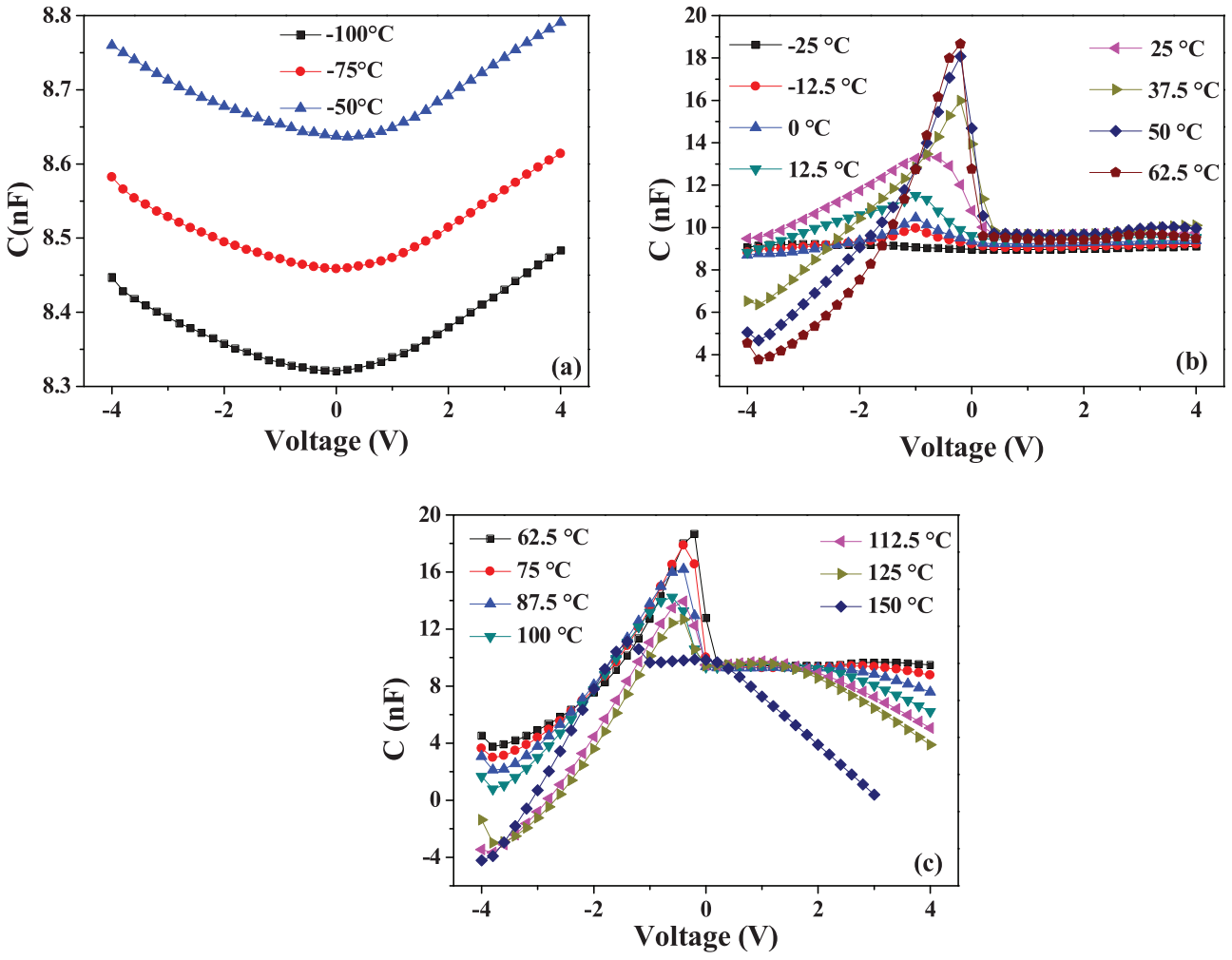

FIG. 1. Capacitance voltage characteristics from 4 to 4 V of Au/TiO_2/Pt/Ti/SiO_2/Si structure at 100 kHz and different temperatures: (a) 100, 75 and 50 °C, (b) from 25 to 62.5 °C, and (c) from 62.5 to 150 °C.

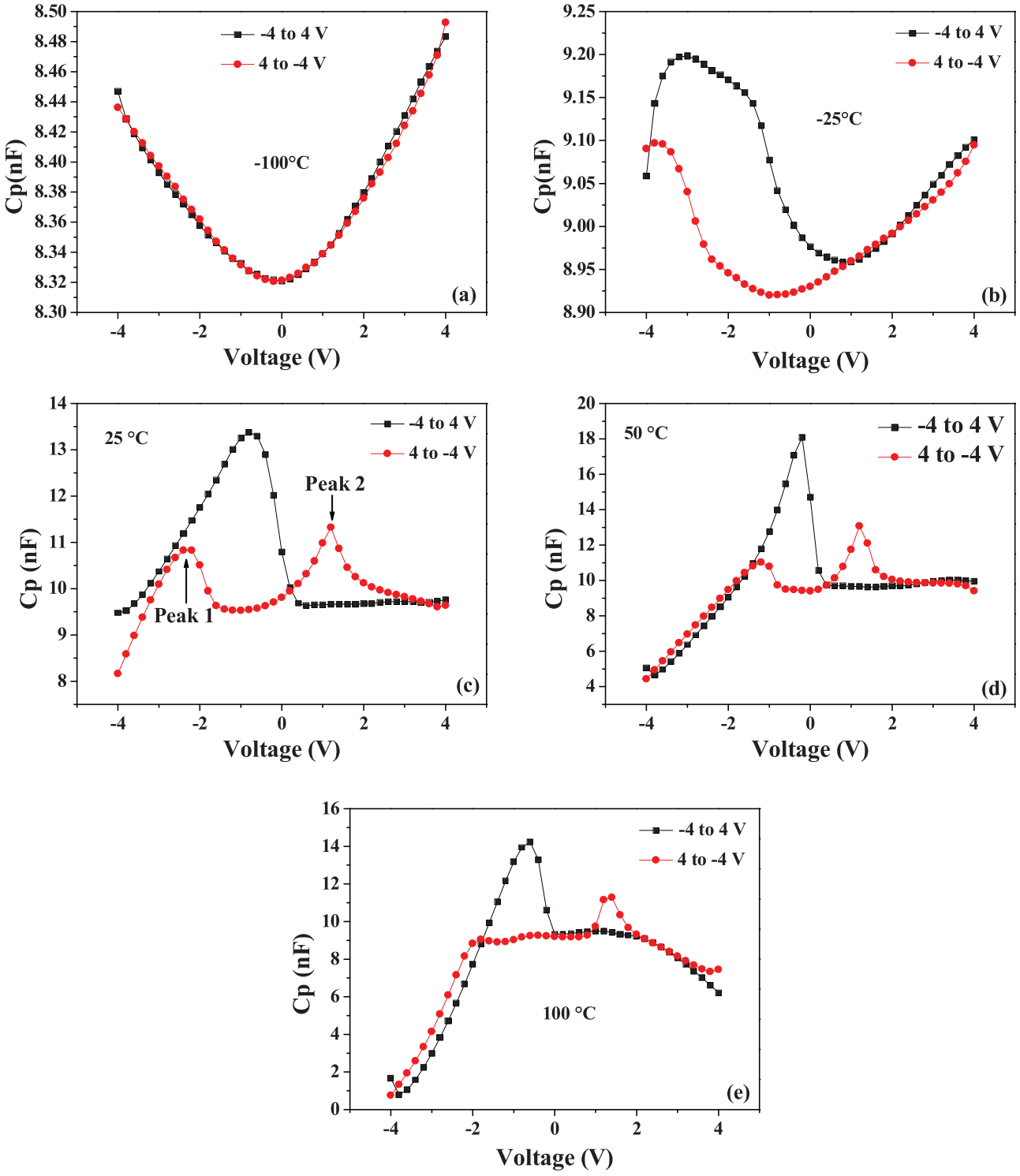

FIG. 2. Reversibility of capacitance voltage characteristics of Au/TiO_2/Pt/Ti/SiO_2/Si structure at 100 kHz and different temperatures: (a) 100 °C, (b) 25 °C, (c) 25 °C, (d) 50 °C, and (e) 100 °C.

phenomenon may result from a dissymmetry in the nature of the electrodes of the MIM capacitor caused by differences in their work functions and the chemistry of the electrode/insulator interface. The appearance of the observed capacitance peaks may relate to the nature of space charges injected from one electrode to another. Indeed, when bias was applied to the Au electrode, one peak was generated, while two appeared when the voltage sweep was reversed (from 4 to −4 V) and bias was applied to the Pt electrode. Peak 1 highlighted in Fig. 2(c) shifted progressively with temperature to lower voltage until its disappearance at 100 °C.

To obtain more insight into the unusual C V behavior, dielectric measurements were performed on the same MIM capacitor structure. Fig. 3(a) shows the frequency dependence of capacitance at temperatures ranging from −150 °C to 160 °C. A plateau, i.e., saturation, independent of the frequency was visible at low frequencies. Its value began to decrease above 80 °C, which may have been related to the

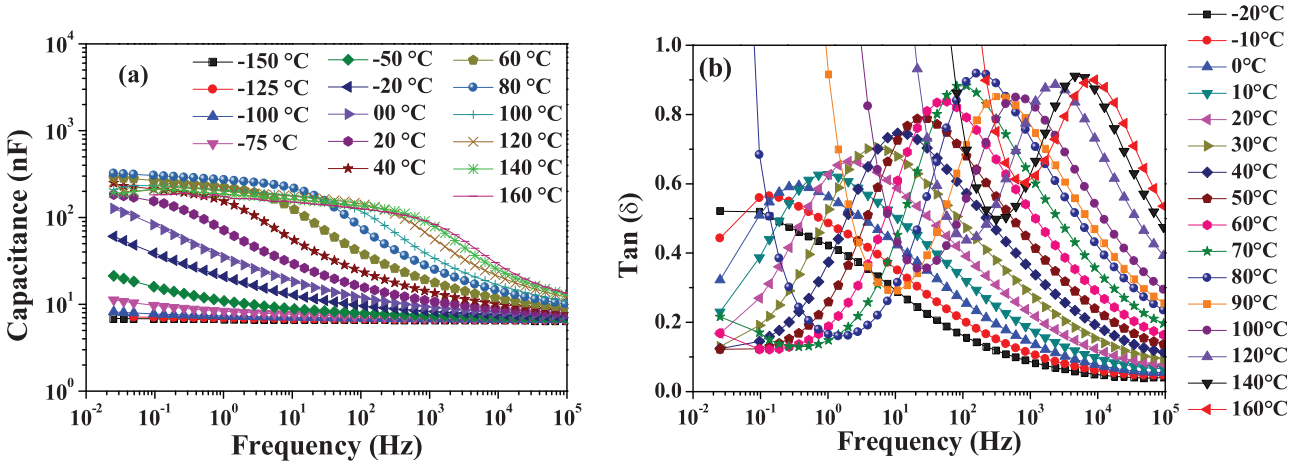

FIG. 3. Frequency dependence of (a) capacitance and (b) dissipation factor at different temperatures.

vanishing of peak 1 in the $C\ V$ characteristics (see Fig. 2(e)). For better understanding of its origin, the dissipation factor is plotted as a function of the frequency in Fig. 3(b). The intensity of the relaxation peak clearly changed at a threshold temperature of 90 °C, in good agreement with the temperature at which the capacitance plateau decreased and peak 1 disappeared in the C-V characteristics.

The Arrhenius plot shown in Fig. 4 indicates an activation energy E_a of 0.65 eV, associated with the relaxation process correlated to the TiO_2 dissipation factor. Various reports have investigated the dominant defect structure in $TiO_{2\ x}$ (where x denotes the non-stoichiometry parameter). At 1000 K, in an x range of 0 0.008 $TiO_{2\ x}$ maintains its rutile, anatase, or brookite phase structure.[22] Outside this x range, the major defects that arise are titanium interstitials (Ti_i) and oxygen vacancies (V_O).[23–26] Both defect types can explain oxygen-deficient non-stoichiometric $TiO_{2\ x}$. The calculated activation energy of 0.65 eV matches that of the first ionization energy of oxygen vacancies ($V_O^{\cdot}$),[27–29] and the ALD TiO_2 relaxation process is mainly attributed to first ionized $V_O^{\cdot}$. This result is in good agreement with other studies that have provided evidence of oxygen vacancies being the major defect type in TiO_2.[30]

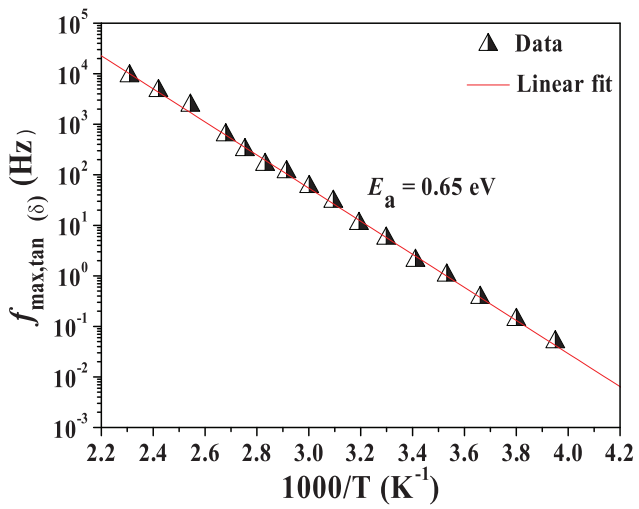

FIG. 4. Arrhenius plot of relaxation process observed in Au/TiO_2/Pt/Ti/SiO_2/Si MIM capacitors.

The frequency dependence of the imaginary part of the electrical modulus (M″) is depicted Fig. 5 to overcome the masking of the relaxation processes that might take place at low frequency by dc conductivity effects. Indeed, this phenomenon cannot be observed using permittivity complex formalism. The appearance of a first relaxation peak at −50 °C was clearly seen at low frequency (Fig. 5(a)). A peak shift to higher frequencies and slight increase in amplitude occurred with increasing temperature to 80 °C. The first peak in the M″ curve (Fig. 5(a)) appeared at the same temperature as that where the first capacitance peak appeared in the negative $C\ V$ range.

From 80 °C, a second relaxation peak (peak 2) appeared and a loss of its symmetrical shape was observed as the temperature was increased owing to the high dc conductivity effect masking the relaxation phenomenon. The temperature range of the second peak in the M″ curve (Fig. 5(b)) is in concordance with that of the observed decrease in the intensity of peak 1 of the capacitance (Fig 1(c)). The relaxation processes are thus well correlated to the capacitance peak/discontinuity ($C\ V$ anomaly).

Furthermore, the Arrhenius plots in Fig. 6 demonstrate that both relaxation peaks (peak 1 and peak 2) obey the Arrhenius law and represent activation energies of 0.6 eV and 1.05 eV, respectively.

Two distinct linear regions are identified in Fig. 7, which presents the dc conductivity of the sample as a function of the inverse temperature at 0.1 Hz. Transition between the regions occurred near 200 °C, and E_a increased from 0.74 eV (low temperature region) to 1.24 eV (high temperature region).

According to the work of Peng,[31] based on first-principle pseudopotential calculations, $V_O^{\cdot\cdot}$ may convert to interstitial titanium, Ti_i, following the reaction:

$$m\mathrm{Ti_{O2}} + 2n\mathrm{V_O^{\cdot\cdot}} \rightarrow (m-n)\mathrm{TiO_2} + n\mathrm{Ti}_i.$$

For consistency, point defects are represented using Kroger-Vink notation.[32] It should be pointed out that six Ti O bonds must be broken to free a titanium atom, while only three are

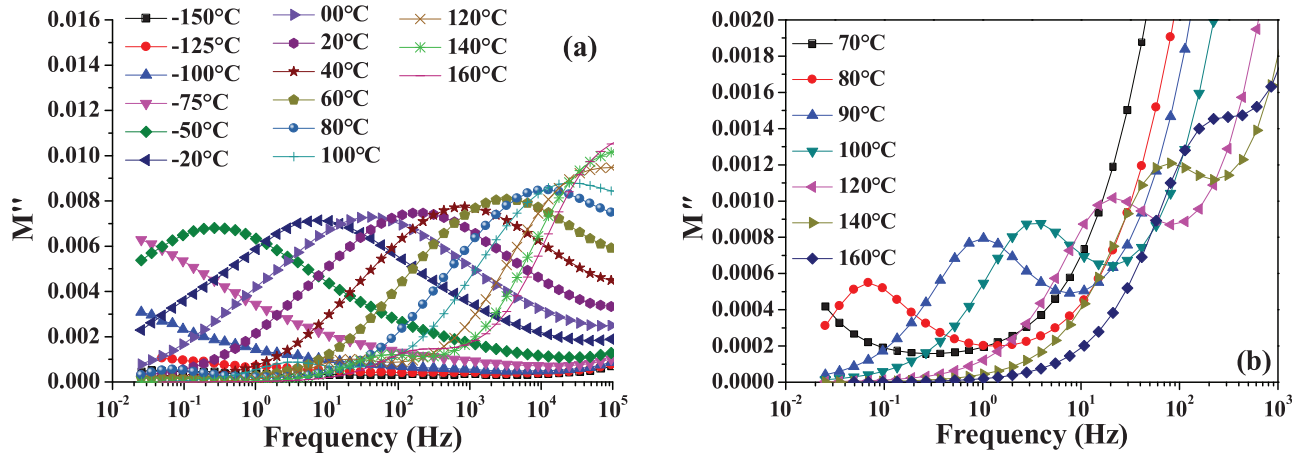

FIG. 5. Imaginary part of the electrical modulus for (a) peak 1 and (b) peak 2 as a function of frequency at different temperatures.

required to free an oxygen atom. Moreover, the number of possible $V_O^{\cdot\cdot}$ sites is double that of Ti_i. From a kinetics point of view, formation of $V_O^{\cdot\cdot}$ is thus more favorable than that of Ti_i, given the same formation energy. The formation energies of $V_O^{\cdot\cdot}$ and Ti_i are very close indeed. Lee *et al.*[33] reported a more complex defect chemistry for TiO_2 than for other wide band gap oxides such as $SrTiO_3$, ZrO_2, and CeO_2. This mainly arises from similar concentrations of two mobile defects, i.e., $V_O^{\cdot\cdot}$ and Ti_i^{3+}, even though some works claim either Ti_i (Refs. 25, 34, and 35) or $V_O^{\cdot\cdot}$ (Refs. 36 and 37) as major defects. The formation mechanisms of such defects may be represented by the following equations.

Interstitial titanium formation is given by

$$(Ti_{Ti})^{\times} + 2O_O{}^{\times} \rightleftharpoons Ti_i^{\cdot\cdot\cdot\cdot} + 4e' + O_2(g).$$

Oxygen vacancy creation is given by

$$O_O{}^{\times} \rightleftharpoons V_O^{\cdot\cdot} + 2e' + 1/2O_2(g).$$

Reoxidation of titanium cations is given by

$$2(Ti_i^{\cdot\cdot\cdot\cdot} - V_O - Ti_i^{\cdot\cdot\cdot\cdot}) + O_2 \rightarrow 2(Ti_i^{\cdot\cdot\cdot\cdot} - O - Ti_i^{\cdot\cdot\cdot\cdot}).$$

Although a few theoretical attempts have previously been made to support experimental results, the origin of the contribution of each defect to the conduction mechanism is discussed here. Comparison with the experimental results is done based on the reports of Cronemeyer[27] and Ghosh *et al.*[28] as well as on recent theoretical results on the energy levels of defect states associated with V_O and Ti_i.[29] According to the literature, oxygen vacancies form two energy levels, at 0.75 eV and 1.18 eV below the conduction band edge, corresponding, respectively, to singly ($V_O^{\cdot}$) and doubly ionized ($V_O^{\cdot\cdot}$) oxygen vacancies. A narrow band at either 1.47 1.56 eV (experimental) or 1.23 eV (theoretical) below the conduction band is also reported. The presence of this band has been tentatively assigned to interstitial Ti_i^{3+} ions. Strunk *et al.*[38] reported the reoxidation of Ti_i^{3+} in Ti_i^{4+} at 200 °C. As previously mentioned, the first (peak 1) and second (peak 2) relaxation peaks can be attributed to the first ($V_O^{\cdot}$) and second ($V_O^{\cdot\cdot}$) ionized oxygen vacancies, respectively. On the other hand, at low temperature, TiO_2 shows a conduction regime governed by electrons from the first ionized oxygen vacancy ($V_O^{\cdot}$) according to the equation: $O^x \rightarrow V_O^{\cdot} + 1/2\ O_2 + 1\ e'$. From 200 °C, the Ti_i^{3+} reoxidation temperature,[38] a regime transition occurs and the conduction mechanism can be attributed to interstitial Ti_i^{3+} ions.

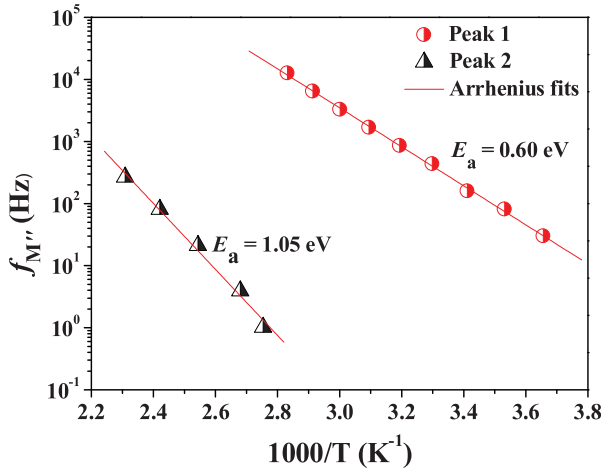

FIG. 6. Arrhenius plots of relaxation processes of TiO_2 obtained from M″.

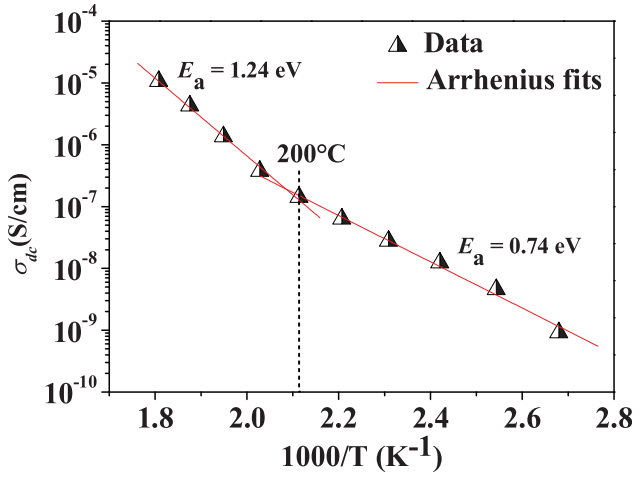

FIG. 7. Arrhenius plots of dc conduction in TiO_2.

IV. CONCLUSION

The correlation between the dielectric and electrical properties of ALD TiO_2 thin films in MIM structures have been investigated to understand their anomalous $C\ V$ response and trap defects. Using electrical correlation, detailed information was obtained about defect levels, anomalous capacitance, and their effects on the dielectric material response of the films. The anomalous $C\ V$ characteristics, observed from $-25\,^{\circ}C$ to high temperature, can be attributed to both defect state dissymmetry at the electrode/dielectric interfaces and ionized oxygen vacancies. Moreover, the two main relaxation processes observed in the M'' plot were associated to the first and second ionized oxygen vacancies, which exhibited corresponding activation energies of 0.60 and 1.05 eV. In contrast, a dc regime transition was found to occur around $200\,^{\circ}C$ that may be correlated to reoxidation of interstitial Ti^{3+} ions. Indeed, an activation energy transition from 0.74 eV (low temperature region) to 1.24 eV (high temperature region) was observed.

As concluded above, traps seem to govern/strongly influence the $C\ V$ response in these materials. In future work, it will thus be necessary to focus on the best protocol that allows us to control the dynamic of charges and traps. Particularly, scans from high temperatures and/or high dc voltages may modify the $C\ V$ response.

[1]A. L. Linsebigler, G. Lu, and J. T. Yates, Jr., Chem. Rev. **95**, 735 (1995).
[2]G. S. Oehrlein, J. Appl. Phys. **59**, 1587 (1986).
[3]L. Messick, J. Appl. Phys. **47**, 4949 (1976).
[4]B. M. Henry, U.S. patent 4, 474 (1978).
[5]M. R. Kozlowski, P. S. Tyler, W. H. Smyrl, and R. T. Atanasoki, J. Electrochem. Soc. **136**, 442 (1989).
[6]M. Lottiaux, C. Boulesteix, G. Nihoul, F. Varnier, F. Flory, R. Galindo, and E. Pelletier, Thin Solid Films **170**, 107 (1989).
[7]K. S. Yeung and Y. W. Lam, Thin Solid Films **109**, 169 (1983).
[8]L. M. Williams and D. W. Hess, J. Vac. Sci. Technol. A **1**, 1810 (1983).
[9]M. Gartner, C. Parlog, and P. Osiceanu, Thin Solid Films **234**, 561 (1993).
[10]M. H. Suhail, G. Mohan Rao, and S. Mohan, J. Appl. Phys. **71**, 1421 (1992).
[11]H. Tang, K. Prasad, R. Sanjines, P. E. Schmid, and F. Levy, J. Appl. Phys. **75**, 2042 (1994).
[12]S. Duenas, H. Castán, H. García, E. San Andrés, M. Toledano Luque, I. Mártil, G. González Díaz, K. Kukli, T. Uustare, and J. Aarik, Semicond. Sci. Technol. **20**, 1044 (2005).
[13]J. Aarik, A. Aidla, T. Uustare, M. Ritala, and M. Leskela, Appl. Surf. Sci. **161**, 385 (2000).
[14]A. Rahtu and M. Ritala, Chem. Vap. Depos. **8**, 21 (2002).
[15]M. Knez, K. Nielsch, and L. Niinisto, Adv. Mater. **19**, 3425 (2007).
[16]M. George, Chem. Rev. **110**, 111 (2010).
[17]G. D. Wilk, R. M. Wallace, and J. M. Anthony, J. Appl. Phys. **89**, 5243 (2001).
[18]E. Rauwel, G. Clavel, M. G. Willinger, P. Rauwel, and N. Pinna, Angew. Chem. Int. Ed. **47**, 3592 (2008).
[19]S. Blonkowski, Appl. Phys. Lett. **91**, 172903 (2007).
[20]J. Koo and H. Jeon, J. Korean Phys. Soc. **46**, 945 (2005).
[21]C. Jorel, C. Vallée, P. Gonon, C. Dubarry, and E. Defay, Appl. Phys. Lett. **94**, 253502 (2009).
[22]K. M. Kim, D. S. Jeong, and C. S. Hwang, Nanotechnology **22**, 254002 (2011).
[23]N. Ait Younes, F. Millot, and P. Gerdanian, Solid State Ionics **12**, 431 (1984).
[24]J. F. Baumard and E. Tani, J. Chem. Phys. **67**, 857 (1977).
[25]R. N. Blumenthal, J. Baukus, and W. M. Hirthe, J. Electrochem. Soc. **114**, 172 (1967).
[26]S. Wendt, P. T. Sprunger, E. Lira, G. K. H. Madsen, Z. Li, J. Ø. Hansen, J. Matthiesen, A. Blekinge Rasmussen, E. Lægsgaard, B. Hammer, and F. Besenbacher, Science **320**, 1755 (2008).
[27]D. C. Cronemeyer, Phys. Rev. **113**, 1222 (1959).
[28]A. K. Ghosh, F. G. Wakim, and R. R. Addiss, Jr., Phys. Rev. **184**, 979 (1969).
[29]F. M. Hossain, G. E. Murch, L. Sheppard, and J. Nowotny, Defect Diffus. Forum **251–252**, 1 (2006).
[30]D. S. Jeong, H. Schroeder, U. Breuer, and R. Waser, J. Appl. Phys. **104**, 123716 (2008).
[31]H. Peng, Phys. Lett. A **372**, 1527 (2008).
[32]F. A. Kroger and H. J. Vink, J. Phys. Chem. Solids **5**, 208 (1958).
[33]D. K. Lee and H. I. Yoo, Solid State Ionics **177**, 1 (2006).
[34]J. F. Baumard, Solid State Commun. **20**, 859 (1976).
[35]J. Sasaki, N. L. Peterson, and K. Hoshino, J. Phys. Chem. Solids **46**, 1267 (1985).
[36]U. Balachandran and N. G. Eror, J. Mater. Sci. **23**, 2676 (1988).
[37]E. H. Greener, F. J. Barone, and W. M. Hirthe, J. Am. Ceram. Soc. **48**, 623 (1965).
[38]J. Strunk, W. C. Vining, and A. T. Bell, J. Phys. Chem. C **114**, 16937 (2010).